

The Porosity and Surface Characteristics of Modified Glass Ionomer Cement

Kemarajt Kemavongse, M.Sc.¹, Nattapon Rotpenpian, D.D.S., Ph.D.²

¹Research and Innovation Development Center, Faculty of Dentistry, Prince of Songkla University, Hat Yai, Songkhla 90110, Thailand.

²Department of Oral Biology and Occlusion, Faculty of Dentistry, Prince of Songkla University, Hat Yai, Songkhla 90110, Thailand.

Received 27 September 2024 • Revised 9 October 2025 • Accepted 10 October 2025 • Published online 20 March 2026

Abstract:

Objective: This study aimed to evaluate the porosity and surface morphology of experimental bioactive glass ionomer cements (BGIC) modified with tricalcium phosphate (TCP), translationally controlled tumor protein (TCTP), and chlorhexidine (CHX). These modifications were intended to enhance the biological and physical performance of conventional glass ionomer cements (GIC) without compromising their structural integrity.

Material and Methods: Six groups of GIC-based materials were prepared (N=8), including unmodified GIC, BGIC, MBGIC, MBGIC+3T, MBGIC+10T, and MBGIC+CHX. Porosity was evaluated using Micro-computed Tomography (Micro-CT) and quantified by calculating pore volume and average pore diameter. Surface morphology was assessed using Scanning Electron Microscopy (SEM) at magnifications of 1,000× and 2,000× to observe the homogeneity, granularity, and presence of voids or cracks.

Results: The BGIC and MBGIC groups exhibited slightly higher porosity values compared to the control GIC group; however, these differences were not statistically significant (p-value=0.947). Similarly, the MBGIC+3T group showed porosity levels comparable to GIC. In contrast, both MBGIC+10T and MBGIC+CHX demonstrated significantly greater porosity than GIC and the lower TCP-modified groups (p-value=0.01), with no significant difference observed between MBGIC+10T and MBGIC+CHX.

Conclusion: Modifications of BGIC with TCP, TCTP, and CHX resulted in increased porosity without compromising the surface integrity or homogeneity of the material. These findings suggest that such modifications could be beneficial in improving ion release and biological activity while maintaining acceptable physical structure. However, the optimal balance between increased porosity and mechanical stability requires further investigation in long-term *in vitro* and *in vivo* studies.

This paper was from the International Dental Collaboration of the Mekong River Region Congress (IDCMR, October 15–17, 2025)
Contact: Assoc.Prof.Dr. Nattapon Rotpenpian, D.D.S., Ph.D.
Department of Oral Biology and Occlusion, Faculty of Dentistry, Prince of Songkla University, Hat Yai, Songkhla 90110, Thailand.
E-mail: nattapon.r@psu.ac.th

J Health Sci Med Res 2026;44(4):e20261338
doi: 10.31584/jhsmr.20261338
www.jhsmr.org

© 2026 JHSMR. Hosted by Prince of Songkla University. All rights reserved.
This is an open access article under the CC BY-NC-ND license
(<http://www.jhsmr.org/index.php/jhsmr/about/editorialPolicies#openAccessPolicy>).

Keywords: Antimicrobial, bioactive materials, glass ionomer cement, micro-CT, porosity, surface morphology

Introduction

Glass ionomer cement (GIC) has been widely utilized in restorative dentistry since its introduction due to its chemical adhesion to dental hard tissues, fluoride-releasing properties, and favorable biocompatibility¹. Its unique setting reaction, which involves an acid-base reaction between polyalkenoic acid and fluoroaluminosilicate glass particles, allows GIC to bond chemically to enamel and dentin, eliminating the need for additional bonding agents². Moreover, the continuous release of fluoride ions provides anti-cariogenic benefits, which are especially valuable in pediatric and geriatric dentistry. Despite these advantages, conventional GIC exhibits several limitations, including relatively low compressive and flexural strength, brittleness, moisture sensitivity during the early setting phase, and the presence of internal porosity, which compromises its mechanical integrity and durability under clinical conditions³.

In response to these challenges, numerous attempts have been made to improve the physical and biological properties of GIC by incorporating bioactive and antimicrobial agents. These efforts have led to the development of bioactive GIC (BGIC) formulations, which aim to enhance the cement's regenerative potential, mechanical strength, and resistance to microbial colonization. One of the commonly studied additives is tricalcium phosphate (TCP), a bioceramic material. It serves as a source of calcium and phosphate ions, which are essential for hydroxyapatite formation and mineralized tissue regeneration. TCP incorporation has shown promise in promoting biomineralization and enhancing dentin bridge formation in vital pulp therapy⁴. However, the inclusion of TCP particles into the GIC matrix may alter its microstructure and porosity profile, thereby affecting not only ion release but also the mechanical stability of the material⁵.

Another promising bioactive agent is translationally controlled tumor protein (TCTP), a multifunctional and highly conserved protein that regulates cell proliferation, differentiation, and apoptosis. TCTP has been shown to modulate inflammatory responses and enhance wound healing, making it a potential candidate for pulp tissue regeneration⁶. However, its impact on the structural characteristics of modified GIC, especially regarding pore architecture and surface integrity, remains largely unexplored. Incorporating TCTP into GIC at different concentrations (e.g., 3 μg and 10 μg) may result in varying biological and physical effects, necessitating further investigation.

In addition to enhancing bioactivity, improving the antimicrobial properties of GIC is also a priority in restorative material design. Chlorhexidine (CHX), a broad-spectrum antimicrobial agent, has been incorporated into dental materials to reduce bacterial colonization and prolong restoration longevity⁷. The integration of CHX into GIC has been reported to reduce microbial adhesion and growth without significantly compromising biocompatibility⁸. Nevertheless, the potential impact of CHX on the internal porosity and surface texture of the cement matrix needs to be carefully evaluated, as it may affect the mechanical and handling properties of the material.

A recent *in vivo* study formulated an enhanced-GIC containing 15% chitosan, 5% bovine serum albumin (BSA), 0.05% TCP, and 1 μg TCTP to evaluate its biocompatibility and regenerative potential in rabbit anterior teeth. Histological analysis after 21 days showed no signs of inflammation or toxicity in the pulp tissue. Instead, the enhanced-GIC group exhibited improved healing potential, as evidenced by increased collagen synthesis and lymphocyte infiltration, suggesting favorable biological interaction with the pulp⁹.

However, while these findings provide insights into the biological effects of modified GIC, little is known about their structural alterations, particularly in terms of porosity and surface changes, which are crucial for the material's mechanical performance and degradation behavior.

To provide a clear comparison of how different bioactive modifications influence the properties of GIC, six representative formulations were selected. Conventional GIC was included as the baseline control, while BGIC served as a biologically enhanced reference. The addition of TCP was intended to enhance remineralization potential, whereas two concentrations of TCTP (3 μg and 10 μg) were chosen to examine the dose-dependent effects on material bioactivity and mechanical integrity. The inclusion of 10% CHX represents an antimicrobial approach designed to broaden clinical applications. This grouping strategy enables a structured evaluation of both individual and combined compositional modifications, supporting a deeper understanding of their effects on material architecture and functionality.

Therefore, the objective of the present study was to investigate and compare the porosity and surface characteristics of six GIC formulations: (1) conventional GIC, (2) BGIC, (3) MBGIC, (4) MBGIC+3T, (5) MBGIC+10T, and (6) MBGIC+CHX. By employing quantitative Micro-CT imaging and surface characterization techniques, this study aimed to provide a comprehensive understanding of how various bioactive additives influence the internal architecture and external morphology of modified GIC, with potential implications for their mechanical performance, clinical longevity, and biological interaction.

Material and Methods

This protocol was reviewed by the Human Research Ethics Committee, Faculty of Dentistry, Prince of Songkla University (EC no: NH6808-017).

Samples preparation

Each modified glass ionomer cement formulation was prepared following the protocol and according to the manufacturer's instructions for GIC, BGIC, MBGIC, MBGIC+3T, MBGIC+10T, and MBGIC+CHX. In this study, three different doses of TCTP (1, 3, and 10 TCTP) were incorporated to establish a dose-response model. The inclusion of 1 TCTP served as a low-dose condition, while 3 TCTP and 10 TCTP represented medium and high doses, respectively. This design enabled evaluation of the effect of TCTP across a range of concentrations, thereby providing a more comprehensive understanding of its dose-dependent behavior. And all the material was instructed by Assoc. Prof. Dr. Ureporn Kedjarune-Leggat and Prof. Dr. Wilaiwan Chotigeat, senior researcher of Prince of Songkla University, Thailand. Additionally, the invention titled "Material for the Release of Substances from Glass Ionomer Cement Modified with Chitosan" was granted a patent on January 31, 2023, under patent number 0501002755 in Thailand. Another related invention, titled "Resin Composition for Application in Glass Ionomer Cement and Its Manufacturing Method," was granted a patent on March 13, 2023, under patent number 1001001095 in Thailand. These patents contribute to advancements in the field of dental materials, specifically enhancing the properties of glass ionomer cement for improved therapeutic outcomes in restorative dentistry. Each sample's composition is illustrated in Table 1.

For a conservative pairwise comparison between any two groups on porosity (the most variable metric). Sample size for each group was estimated using the following formula¹⁰:

$$n = [2 \times \sigma^2 \times (Z_{(1-\alpha/2)} + Z_{(1-\beta)})^2] / \Delta^2$$

where:

σ^2 =variance (based on previous data for GIC materials)

Δ =minimum detectable difference (set at 3% absolute difference in porosity)

$Z(1-\alpha/2)=1.96$ for a two-sided significance level of $\alpha=0.05$

$Z(1-\beta)=0.84$ for 80% power

Sample size was calculated by substituting $\sigma=2\%$ (variance=4), $\Delta=3\%$, $Z(1-\alpha/2)=1.96$, and $Z(1-\beta)=0.84$. The required sample size was approximately 7 specimens per group¹¹. To account for potential specimen loss and to maintain balanced group sizes, the final sample size was set at 8 specimens per group (total N=48).

Method of Micro-CT scan

The study assessed porosity using micro-computed tomography (Micro-CT) at the micrometer level after the samples were soaked in water for 14 days. The results were expressed as the ratio of bone volume to total volume (BV/TV). This ratio was then used to calculate the percentage of pores in the samples using the formula:

$$\text{Porosity}(\%) = \frac{1 - BV}{TV} \times 100$$

BV=Bone volume or volume of voids , TV=Total volume

After each modified glass ionomer cement formulation was prepared as described above, the specimens were scanned using a high-resolution micro-computed tomography system (MicroCT35; SCANCO Medical,

Bassersdorf, Switzerland). Scanning was performed at 70 kVp, 114 μ A, and 8 W power, with an integration time of 800 ms. The scans were conducted at an isotropic voxel size of 15 μ m to ensure accurate resolution of internal microstructures. A total of 1000 projections were acquired over a 360° rotation using a cone-beam geometry. The raw projection data were reconstructed using a filtered back-projection algorithm to produce axial cross-sectional images. The reconstructed datasets were exported as 16-bit grayscale images at a resolution of 1024 \times 1024 pixels. Image processing and quantitative analysis were performed using Scanco Evaluation Software, including segmentation by global thresholding to isolate voids from solid phases. Parameters such as total porosity (%), pore volume, and pore size distribution were calculated within a defined cylindrical region of interest (ROI). 3D volume rendering was additionally performed for qualitative assessment of surface morphology.

Surface morphology analysis using scanning electron microscopy (SEM)

The surface morphology of the modified glass ionomer cement (GIC) specimens was examined using scanning electron microscopy (SEM) to assess the topographical changes resulting from various additive

Table 1 Composition of glass ionomer cements used in the study

Glass ionomer	Composition
GIC	100% of glass ionomer cement powder
BGIC	80% of glass ionomer cement powder, 15% of chitosan, and 5% of bovine serum albumin
MBGIC	79.95% of glass ionomer cement powder, 15% of chitosan, 5% of bovine serum albumin, and 0.05% of tricalcium phosphate and 1 μ g Pmer-TCTP (added when mixing the powder and liquid components)
MBGIC+3T	79.95% of glass ionomer cement powder, 15% chitosan, 5% of bovine serum albumin, 0.05% of tricalcium phosphate, and 3 μ g Pmer-TCTP (added when mixing the powder and liquid components)
MBGIC+10T	79.95% of glass ionomer cement powder, 15% chitosan, 5% of bovine serum albumin, 0.05% of tricalcium phosphate, and 10 μ g Pmer-TCTP (added when mixing the powder and liquid components)
MBGIC+CHX	79.95% of glass ionomer cement powder, 15% chitosan, 5% of bovine serum albumin, 0.05% of tricalcium phosphate, and 1 μ g Pmer-TCTP+10% chrohexidine

incorporations. Disk-shaped samples (6 mm in diameter and 2 mm in thickness) were prepared for each experimental group, including: (1) conventional GIC (control), (2) BGIC, (3) MBGIC, (4) MBGIC+3T, (5) MBGIC+10T, and (6) MBGIC+CHX.

After setting, all specimens were stored in 100% humidity at 37°C for 24 hours to ensure complete setting. The samples were then rinsed with distilled water and air-dried at room temperature. To prepare the specimens for SEM observation, each sample was mounted onto aluminum stubs using double-sided carbon adhesive tape. The samples were then sputter-coated with a thin layer of gold-palladium alloy (approximately 10–15 nm thickness) using a sputter coater (e.g., JEOL JFC-1600, Japan) to enhance conductivity.

Surface images were captured using a field emission scanning electron microscope (e.g., JEOL JSM-IT300, Japan) operated at an accelerating voltage of 10–15 kV. Images were obtained at various magnifications (typically $\times 500$, $\times 1,000$, and $\times 5,000$) to evaluate surface texture, particle distribution, voids, and microstructural features of the material surface¹². Representative images from three independent specimens per group were recorded and qualitatively compared.

Statistical analysis

All data are presented as means and standard deviations (S.D.). The normality of the data distribution was assessed using the Shapiro–Wilk test, which confirmed a normal distribution in this study. One-way ANOVA, followed by Tukey's multiple comparison test, was performed to evaluate the differences among groups, with the significance level set at $\alpha=0.05$.

Results

Micro-CT evaluation

Quantitative analysis of porosity using high-resolution

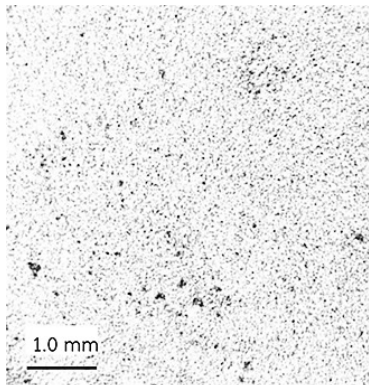
micro-computed tomography revealed distinct differences among the experimental groups (Figure 1). The GIC group exhibited the lowest porosity (~14%), serving as the baseline reference. BGIC, MBGIC, and MBGIC+3T showed slightly higher porosity compared with GIC; however, these differences were not statistically significant (p -value=0.947). In contrast, MBGIC+10T and MBGIC+CHX demonstrated significantly greater porosity (~22–27%) compared with GIC and the lower TCP-modified groups (p -value=0.01). No significant difference was observed between MBGIC+10T and MBGIC+CHX ($p=0.976$), as shown in Figure 2.

Table 2 Average pore-size diameter of the samples from different groups

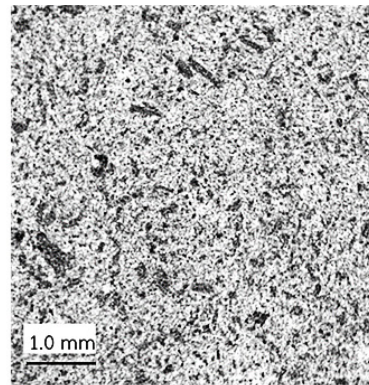
Group	Pore-size diameter Mean \pm S.D. (mm)
GIC	0.053 \pm 0.01 ^a
BGIC	0.136 \pm 0.04 ^b
MBGIC	0.076 \pm 0.01 ^a
MBGIC+3T	0.082 \pm 0.01 ^a
MBGIC+10T	0.173 \pm 0.02 ^c
MBGIC+CHX	0.150 \pm 0.02 ^{b,c}

One-way ANOVA with Tukey multiple comparison test. Statistical groupings (^a, ^b, ^c) indicate that specimens labeled with the same superscript letter are not significantly different (p -value>0.05), S.D.=standard deviations

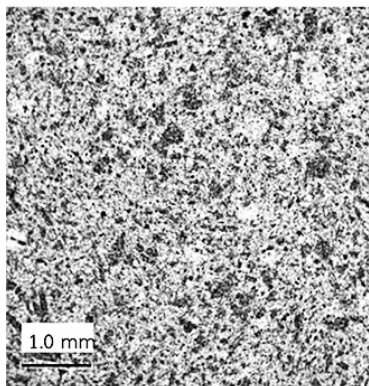
For the average pore size diameter (Table 2), the MBGIC+10T group exhibited the largest pore size (0.173 \pm 0.02 mm), which was not significantly different from MBGIC+CHX (0.150 \pm 0.02 mm; p -value=0.876). The BGIC group (0.136 \pm 0.04 mm) showed a significantly larger pore size compared with GIC (0.053 \pm 0.01 mm; p -value=0.028), indicating that the incorporation of bioactive glass increased pore size. The addition of 3T to MBGIC (0.082 \pm 0.01 mm) did not produce a significant difference from the control MBGIC group (0.076 \pm 0.01 mm; p -value=0.876). In contrast, MBGIC+10T (0.173 \pm 0.02 mm) demonstrated a significantly larger pore size compared with MBGIC (p -value=0.035). Similarly, MBGIC+CHX (0.150 \pm 0.02 mm)



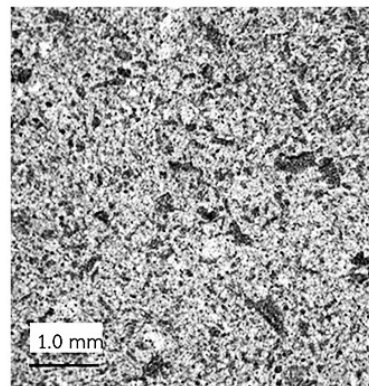
GIC



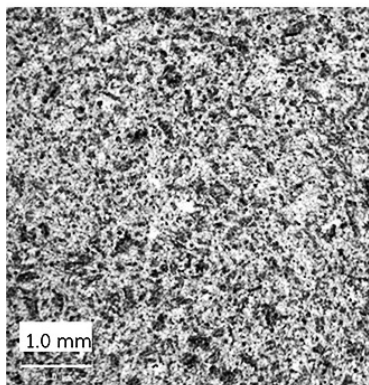
BGIC



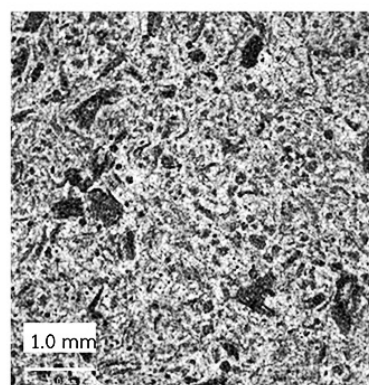
MBGIC



MBGIC + 3T



MBGIC + 10T



MBGIC+CHX

Figure 1 Micro-CT evaluation of sample microstructures at 15 μ m voxel size (70 kVp, 114 μ A, 8 W, 800 ms)

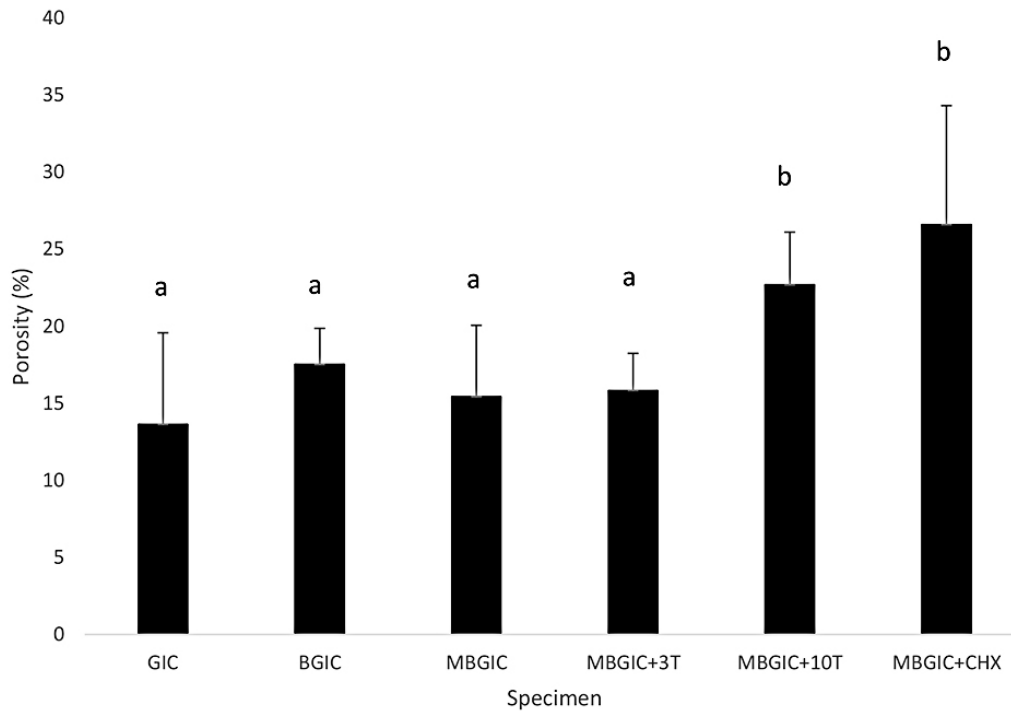


Figure 2 Mean percentage of porosity analyzed by Micro-CT X-ray at a voxel size of 15 μm (70 kVp, 114 μA , 8 W, 800 ms integration time)

exhibited a significantly larger pore size than GIC, MBGIC, and MBGIC+3T (p -value=0.039).

The determination of surface morphology using SEM

The surface morphology of the different experimental groups was observed using SEM, and representative micrographs are presented in Figure 3. All groups, including the unmodified GIC and the various formulations (BGIC, MBGIC, MBGIC+3T, MBGIC+10T, and MBGIC+CHX), demonstrated relatively homogeneous surfaces without evident cracks, large voids, or irregular porosities.

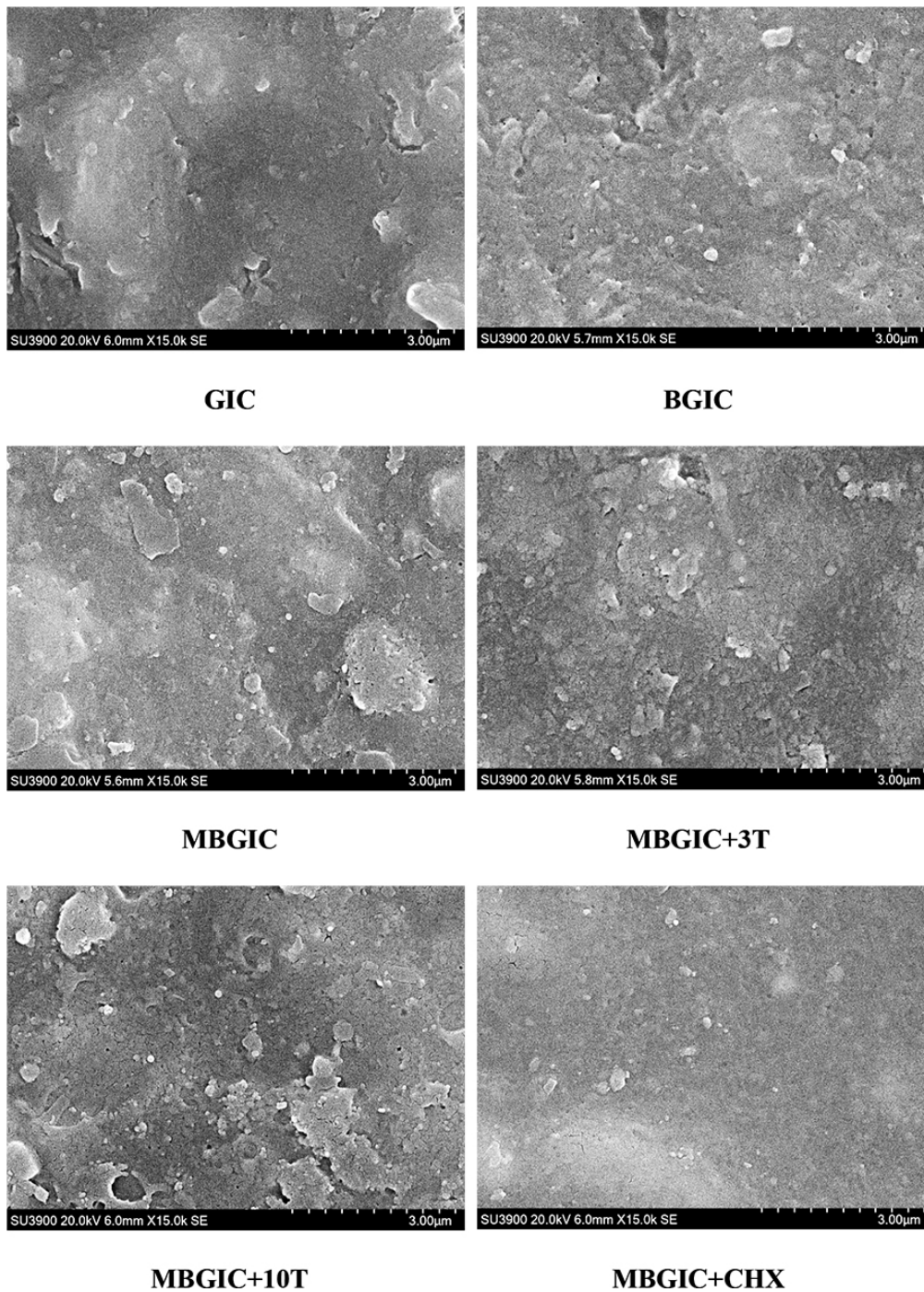
The control GIC group displayed a smooth surface with minimal granular texture. The Bio-GIC group exhibited slightly rougher surfaces, but no apparent structural disruption was observed. Similarly, the incorporation of TCP

and TCTP at both 3 μg and 10 μg concentrations, and 10% CHX into the BGIC matrix did not result in any remarkable differences in surface topography when compared with the control groups.

Overall, there were no significant visual differences in surface morphology among the groups. All samples maintained consistent particle distribution and surface integrity under SEM at the magnifications examined.

Discussion

In recent years, the advancement of restorative dental materials has shifted towards the development of bioactive and biocompatible formulations to enhance tissue healing and minimize inflammatory responses. GIC, a widely used restorative material, has been modified with bioactive additives to improve its physicochemical and biological



Data are presented as mean±standard deviation (S.D.). Statistical comparisons were performed using one-way analysis of variance (ANOVA) followed by Tukey's post hoc test. Groups labeled with different superscript letters differ significantly at p-value<0.05.

Figure 3 Scanning Electron Microscopy at 5,000xmagnification of GIC, BGIC, MBGIC, MBGIC+3T, MBGIC+10T, and MBGIC+CHX

performance. In this study, the incorporation of TCP, TCTP, and CHX into the BGIC matrix was investigated to evaluate the effects on porosity and surface morphology. The findings provide critical insights into how these modifications influence the microstructural characteristics of the material, which are essential determinants of its performance in clinical settings.

Porosity is a crucial parameter in dental materials as it directly affects mechanical properties, water absorption, degradation rate, and ion release profiles¹³. Excessive porosity can compromise the material's mechanical strength, increase susceptibility to microleakage, and promote bacterial colonization¹⁴. Conversely, controlled porosity may facilitate ion exchange and enhance bioactivity. In the present study, the Micro-CT analysis revealed that the BGIC+TCP and MBGIC groups exhibited higher porosity values compared to the unmodified GIC control group, with a relative ratio of 1.71:1. Among the experimental formulations, MBGIC demonstrated the highest porosity level, suggesting that the incorporation of TCP at this concentration alters the matrix structure to a more open configuration.

The increase in porosity observed in TCP-containing groups is likely due to the particulate nature of TCP, which may interfere with the uniform setting reaction of the GIC matrix. Previous studies have shown that the addition of calcium phosphates, including hydroxyapatite and β -TCP, can result in increased void formation during mixing and setting, due to agglomeration or poor wetting of particles by the polyacrylic acid component¹⁵. Furthermore, the calcium ions released from TCP may compete with the cations in the GIC setting process, leading to a less dense cross-linked matrix and subsequently higher porosity¹⁶.

Despite the increase in overall porosity, the average pore size in the MBGIC group was significantly smaller than that of the control group, with statistical significance (p -value<0.05). This suggests a more refined microstructure with numerous small pores rather than fewer large voids.

This pattern is favorable in terms of ion release and bioactivity, as small interconnected pores can facilitate diffusion while maintaining mechanical integrity¹⁷. Such findings indicate that the material may support controlled ion leaching, such as fluoride and calcium, which are beneficial for remineralization and antibacterial properties.

The surface morphology analysis via SEM offers complementary insights into the microstructure of restorative materials. In this study, SEM micrographs showed relatively homogenous surfaces across all the tested groups without evident cracks, large voids, or structural disruptions. The control GIC group presented with a smooth surface and minimal granular texture, consistent with prior studies describing its dense, glassy appearance due to the presence of unreacted glass particles embedded in a siliceous hydrogel matrix¹⁸.

The BGIC group, which incorporates additional biopolymers, exhibited a slightly rougher surface. However, this increased roughness did not compromise surface integrity. This may be attributed to the interaction between biopolymers and the polyacrylic acid, potentially altering the gelation dynamics and surface energy of the set cement. These changes could promote better adhesion or integration with biological tissues, although further *in vivo* testing would be necessary to confirm such hypotheses.

The experimental groups modified with TCP, TCTP (3 μ g and 10 μ g), and 10% CHX did not display remarkable differences in surface morphology compared to the unmodified GIC or BGIC. All groups maintained consistent particle distribution and surface continuity under SEM at the tested magnifications. These results suggest that the addition of these agents, at the tested concentrations, does not negatively impact the surface characteristics of the GIC-based formulations.

It is noteworthy that despite the increased porosity observed in the Micro-CT analysis of TCP-modified groups, this was not clearly reflected in the SEM images.

This discrepancy could be due to the limitations of surface imaging compared to volumetric analysis. While SEM provides high-resolution surface detail, it may not detect internal or subsurface porosities unless cross-sectional views are utilized. This reinforces the importance of using complementary techniques such as Micro-CT for comprehensive evaluation. Overall, Micro-CT analysis revealed that the incorporation of TCP, at both low and high concentrations, did not significantly alter the porosity of Bio-GIC when compared with the unmodified material. In contrast, the addition of 10% chlorhexidine substantially increased porosity, reaching values above 26%, which were significantly higher than GIC, BGIC, and all TCP-modified groups. These findings indicate that while TCP incorporation maintains structural integrity comparable to conventional formulations, chlorhexidine loading compromises the microstructural density of the cement.

Tricalcium phosphate is a bioactive ceramic known for its osteoconductive properties and ability to release calcium and phosphate ions, which promote remineralization and cellular responses¹⁹. The observed increase in porosity upon TCP incorporation may be a double-edged sword. While beneficial for ion exchange, it could potentially compromise mechanical properties if not properly controlled. However, the smaller pore size in MBGIC suggests that the formulation maintains structural refinement, which could support its use in minimally loaded clinical applications such as liner or base materials in atraumatic restorative treatment (ART).

Previous studies have reported enhanced remineralization and pulp healing when TCP was incorporated into resin- or GIC-based materials⁹. These biointeractive properties are particularly desirable in pediatric and geriatric dentistry, where pulp vitality preservation is crucial. However, further studies are warranted to assess the long-term durability and mechanical stability of the porous structure observed.

The incorporation of TCTP at both 3 µg and 10 µg concentrations did not significantly alter the surface morphology of the BGIC formulation. TCTP is a multifunctional protein involved in cell proliferation, apoptosis inhibition, and tissue regeneration⁷. The integration of TCTP into a GIC matrix represents a novel strategy aimed at enhancing the material's regenerative potential. Despite its biochemical activity, TCTP at the tested levels did not interfere with the surface structure, suggesting good compatibility with the cement matrix.

Chlorhexidine, a broad-spectrum antimicrobial agent, was incorporated at 10% concentration into BGIC. Similar to TCTP, CHX did not induce significant changes in surface appearance. This is consistent with prior studies that reported the successful incorporation of CHX into GIC without compromising surface smoothness or microstructural integrity²⁰. However, it is essential to monitor the potential impact of CHX on the mechanical properties and fluoride release behavior in future evaluations.

The overall findings indicate that BGIC formulations, modified with TCP, TCTP, and CHX, maintain acceptable surface morphology while exhibiting tailored porosity profiles. These characteristics are critical for clinical performance, especially in terms of material-tissue interactions, sealing ability, ion release, and potential remineralization²¹.

The increased porosity in the MBGIC group, coupled with a smaller average pore size, may create a favorable environment for ion exchange and tissue integration. Such a formulation could be advantageous in vital pulp therapy, where bioactivity is desired over compressive strength. The maintenance of surface integrity across all formulations supports the feasibility of incorporating biological or antimicrobial agents into GIC matrices without compromising handling or esthetic properties.

Further investigations are warranted to examine the correlation between porosity and mechanical performance (e.g., compressive strength, microhardness), as well as to evaluate the biological responses *in vitro* and *in*

vivo. Additionally, long-term leaching studies and aging simulations should be conducted to assess the durability of the modified materials.

From a translational perspective, these findings support the development of next-generation biointeractive GIC that combine the traditional benefits of fluoride release and chemical adhesion with regenerative and antimicrobial functionalities. Such multifunctional materials align with the current trends in minimally invasive and biologically oriented dentistry.

Conclusion

The modification of BGIC, MBGIC, MBGIC+3T, MBGIC+10T, and MBGIC+CHX resulted in notable changes in surface characteristics, particularly an increase in porosity, while maintaining overall surface integrity and homogeneity. The enhanced porosity may be attributed to certain proportions interfering with the composition; however, the surface characteristics remain similar to those of conventional GIC.

Acknowledgement

We appreciate and thank Assoc.Prof.Dr. Urepor Kedjarune-Leggat and Prof.Dr. Wilaiwan Chotigeat, senior researcher at Prince of Songkla University, Thailand, for the materials and methods of this study. We appreciate and thank the Research and Innovation Development Center, Faculty of Dentistry, for its facility support.

Conflict of interest

No conflict of interest.

References

1. Danelon M, Nunes GP, Sterzenbach T, Hannig C. Enhancing antimicrobial properties of glass ionomer cement through metallic agent reinforcement: a systematic review and meta-analysis. *J Dent* 2025;160:105892. doi: 10.1016/j.jdent.2025.105892.
2. Durrant L, Mutahar M, Daghreery AA, Albar NH, Alwadai GS, Alqahtani SA, et al. Clinical performance of glass ionomer

3. Moberg M, Brewster J, Nicholson J, Roberts H. Physical property investigation of contemporary glass ionomer and resin-modified glass ionomer restorative materials. *Clin Oral Investig* 2019;23:1295-308. doi: 10.1007/s00784-018-2554-3.
4. Viswanathan N, Kumar IA, Meenakshi S. Development of chitosan encapsulated tricalcium phosphate biocomposite for fluoride retention. *Int J Biol Macromol* 2019;133:811-6. doi: 10.1016/j.ijbiomac.2019.04.076.
5. Khan AS, Syed MR. A review of bioceramics-based dental restorative materials. *Dent Mater J* 2019;38:163-76. doi: 10.4012/dmj.2018-039.
6. Wanachottrakul N, Chotigeat W, Kedjarune-Leggat U. Effect of novel chitosan-fluoroaluminosilicate resin modified glass ionomer cement supplemented with translationally controlled tumor protein on pulp cells. *J Mater Sci Mater Med* 2014;25:1077-85. doi: 10.1007/s10856-013-5137-5.
7. Jitpukdeebodintra S, Tannukit S, Rotpenpian N. Antimicrobial potential and biological properties of modified glass-ionomer cement supplemented with chlorhexidine diacetate. *J Oral Sci* 2025;67:146-51. doi: 10.2334/josnurd.25-0068.
8. Ratnayake J, Veerasamy A, Ahmed H, Coburn D, Loch C, Gray AR, et al. Clinical and microbiological evaluation of a chlorhexidine-modified glass ionomer cement (GIC-CHX) restoration placed using the atraumatic restorative treatment (ART) technique. *Materials (Basel)* 2022;15. doi: 10.3390/ma15145044.
9. Rotpenpian N, Sornying P, Manmoo S, Dejyong K. Enhanced glass ionomer cement with bioactive additives for collagen synthesis and inflammation in pulp-rabbit teeth. *J Oral Biol Craniofac Res* 2025;15:1021-8. doi: 10.1016/j.jobcr.2025.07.007.
10. Charan J, Biswas T. How to calculate sample size for different study designs in medical research. *Indian J Psychol Med* 2013; 35:121-6. doi: 10.4103/0253-7176.116232
11. Jordáki D, Veress V, Kiss T, Szalma J, Fráter M, Lempel E. Comparative micro-CT analysis of internal adaptation and closed porosity of conventional layered and thermoviscous bulk-fill resin composites using total-etch or universal adhesives. *Polymers* 2025;17:2049. doi: 10.3390/polym17152049.
12. Kalantar Motamedi MR, Mortaheb A, Zare Jahromi M, Gilbert BE. Micro-CT evaluation of four root canal obturation techniques. *Scanning* 2021;6632822. doi: 10.1155/2021/6632822.

13. Sarna-Boš K, Skic K, Sobieszcański J, Boguta P, Chalas R. Contemporary approach to the porosity of dental materials and methods of its measurement. *Int J Mol Sci* 2021;22. doi: 10.3390/ijms22168903.
14. Zhevtun I, Gordienko P, Kulchin Y, Nikitin A, Pivovarov D, Yarusova S, Golub A, Nikiforov P, Timchenko V. Influence of titanium surface porosity on adhesive strength of coatings containing calcium silicate. *Materials (Basel)* 2020;13. doi: 10.3390/ma13204493.
15. Jalili K, Abbasi, F, Oskoe SS, Alinejad Z. Relationships between the morphology, swelling and mechanical properties of poly(dimethyl siloxane)/poly(acrylic acid) interpenetrating networks. *J Mech Behav Biomed Mater* 2009;2:534–41. doi: 10.1016/j.jmbbm.2009.01.002.
16. Vilela HS, Trinca RB, Alves TVM, Scaramucci T, Sakae LO, Mariano F S, Giannini M, Silva FRO, Braga RR. Effect of a calcium silicate cement and experimental glass ionomer cements containing calcium orthophosphate particles on demineralized dentin. *Clin Oral Investig* 2024;28:97. doi: 10.1007/s00784-024-05489-6.
17. Taghvaei N, Ghavami-Lahiji M, Evazalipour M, Tayefeh Davaloo R, Zamani E. Ion release, biocompatibility, and bioactivity of resin-modified calcium hydroxide cavity liners. *BMC Oral Health*. 2023;23:1034. doi: 10.1186/s12903-023-03723-3.
18. Tay FR, Pashley EL, Huang C, Hashimoto M, Sano H, Smales RJ, Pashley DH. The glass-ionomer phase in resin-based restorative materials. *J Dent Res*. 2001;80:1808–12. doi: 10.1177/00220345010800090701.
19. Silva-Barroso AS, Cabral CSD, Ferreira P, Moreira AF, Correia IJ. Lignin-enriched tricalcium phosphate/sodium alginate 3D scaffolds for application in bone tissue regeneration. *Int J Biol Macromol* 2023;239:124258. doi: 10.1016/j.ijbiomac.2023.124258.
20. Sangsuwan P, Chotigeat W, Tannukit S, Kedjarune-Leggat U. Long-term effect of modified glass ionomer cement with mimicked biological property of recombinant translationally controlled protein. *Polymers (Basel)* 2022;14. doi: 10.3390/polym14163341.
21. Chumpraman A, Tannukit S, Chotigeat W, Kedjarune-Leggat U. Biocompatibility and mineralization activity of modified glass ionomer cement in human dental pulp stem cells. *J Dent Sci* 2023;18:1055–61. doi: 10.1016/j.jds.2022.11.024.